

# Enhancing Alzheimer’s Disease Diagnosis Records with Large Language Models: A Pipeline for Multimodal and Longitudinal EHRs

Anonymous ACL submission

## Abstract

Alzheimer’s disease (AD) is a neurodegenerative, incurable condition and a leading cause of morbidity among individuals over 65 in the US. The screening and early diagnosis of AD condition is usually based on the patient’s electrical health records (HERs), including clinical observations, cognitive tests, patient profiles, and medical-imaging-aided diagnoses. However, above information for researchers is highly fragmented. One of the most critical clinical diagnostic notes is stored in structured tables using specialized terminological formats. This presents significant challenges to the accessibility and readability for non-experts, thereby hindering information processing and the development of general medical AI systems. This work proposes a novel pipeline for processing AD clinical diagnostic information: (1) we collect clinical data from the largest AD dataset of Alzheimer’s Disease Neuroimaging Initiative (ADNI)<sup>1</sup>, explain abbreviations and terminology, and organize the information in an accessible manner for those without expert knowledge of AD. (2) Leveraging the power of Large Language Models (LLMs), we present a GPT-based method that effectively transforms tabular clinical data into fluent and faithful natural language diagnostic reports, as demonstrated by our experimental results. (3) We further explore the inherently multi-modal nature of medical data, collecting and processing a total of 10387 volumetric T1-weighted MRI scans from ADNI. (4) Finally, we discuss the existing limitations in applying multimodality EHRs for brain disease analysis and propose forward-looking directions to meet the demands of the neuroimaging domain. We expect that this work will provide new insights into the neuroimaging domain and improve AI applications in healthcare. Our code is available at <https://anonymous.4open.science/r/ADNI-table-to-Text-2EDB>

Participant_ID			clinical Description Reference
Attribute	Value		
Basic Personal information	Age	72.0	<b>Basic Personal Information:</b> Subject 098_S_0896 is a 72.0-year-old Female who has completed 15 years of education. The ethnicity is Not Hisp/Latino and race is White. Marital status is Married. Initially diagnosed as AD, as of the date 2007-10-24, the final diagnosis was Dementia.
	Sex	Female	
	Education	15	
	Race	White	
	DX_bi	AD	
Biomarker measurements	DX	Dementia	<b>Biomarker Measurements:</b> The subject’s genetic profile includes an ApoE4 status of 0.0...
	...	...	
	APOE4	1.0	
Cognitive and neurofunctional Assessments	TAU	212.5	<b>Cognitive and Neurofunctional Assessments:</b> The Mini-Mental State Examination score stands at 29.0. The Clinical Dementia Rating, sum of boxes, is 1.0. ADAS 11 and 13 scores are 4.67 and 4.67 respectively, with a score of 1.0 in delayed word recall...
	...	...	
	MMSE	29.0	
Volumetric data	CDRSB	0.0	<b>Volumetric Data:</b> Under MRI conditions at a field strength of 1.5 Tesla MRI Tesla, using Cross-Sectional FreeSurfer (FreeSurfer Version 4.3), the imaging data recorded includes ventricles volume at 54422.0, hippocampus volume at 6677.0, whole brain volume at 1147980.0, entorhinal cortex volume at 2782.0, fusiform gyrus volume at 19432.0, and middle temporal area volume at 24951.0. The intracranial volume measured is 1799580.0....
	...	...	
	FLDSTRENG	1.5 Tesla MRI	
	Ventricles	84599	
	Hippocampus	5319	
...	...		

Figure 1: An example of a clinical notes

## 1 Introduction

Alzheimer’s disease (AD) is a progressive neurodegenerative disorder characterized by a continuum that ranges from undetectable brain changes to significant alterations that impair memory, culminating in severe physical disabilities(Aramadaka et al., 2023). Current research suggests that the clinical stages of AD can be divided into three stages(Frisoni et al., 2010; Jack et al., 2010). First is the pre-symptomatic phase, where individuals are cognitively normal despite having AD pathological changes. The second phase is the prodromal phase, often referred to as mild cognitive impairment (MCI), characterized by the onset of early cognitive symptoms. The third phase is dementia, marked by severe impairments across multiple domains, leading to loss of function(Yu et al., 2023). The pathological changes in the pre-symptomatic phase may begin to develop decades before the earliest clinical symptoms appear in the prodromal phase. While there is currently no cure for AD once established, in the realm of machine learning and deep learning, differentiating AD from the prodromal stage is a significant issue that interests a large amount of researchers making efforts on(Miller et al., 2022; Zhou et al., 2023b; Cai et al., 2023; Feng et al., 2023; Leng et al., 2023; Liang et al., 2023; Zhou et al., 2023a; Zhang et al., 2023).

<sup>1</sup><https://adni.loni.usc.edu/>

071 Previous studies have predominantly focused on  
072 analyzing medical brain images like Magnetic Res-  
073 onance Imaging (MRI) scans and Position Emis-  
074 sion Tomography (PET) solely, extracting various  
075 features and designing algorithms to diagnose AD  
076 and MCI. The recently revised clinical criteria for  
077 detecting AD emphasize the importance of using  
078 multiple modalities such as core biomarkers and  
079 clinical tests for diagnosis(Carrillo and Masliah,  
080 2023). However, much of this information has  
081 not yet been incorporated into brain disease stud-  
082 ies. Thanks to the widespread implementation of  
083 EHRs, a rich array of routine clinical reports about  
084 participants are digitally available in a tabular form  
085 and offered by the Alzheimer’s Disease Neuroimag-  
086 ing Initiative (ADNI)(Jack Jr et al., 2008). These  
087 tabular datasets offer rich details including demo-  
088 graphic attributes, biomarker measurements, cog-  
089 nitive and neurofunctional assessments, and image  
090 information, making it an invaluable resource.

091 Despite their potential, the complexity of medi-  
092 cal terminology often makes EHRs less accessible  
093 to non-professionals, limiting their utility. While  
094 ADNI ERHs provide complementary information  
095 except for medical scans for understanding disease  
096 patterns, for example, early researches report that  
097 age is the single most significant risk factor for AD  
098 and a higher incidence of MCI occurs in females  
099 than in males(Aramadaka et al., 2023; Katz et al.,  
100 2012), there is an urgent need to develop method-  
101 ologies that can simplify and harness this wealth  
102 of information.

103 As an essential and widely used data format,  
104 tabular data plays a crucial role in structuring in-  
105 formation, significantly advancing the fields of in-  
106 formation retrieval and knowledge extraction for  
107 data mining(Engelmann et al., 2023; 10., 2022; Sui  
108 et al., 2023). Recently, LLM based on the Trans-  
109 former architecture(Vaswani et al., 2017) have be-  
110 come increasingly prominent in addressing a wide  
111 range of natural language-related tasks. Given  
112 their state-of-the-art performance and board ap-  
113 plication potential, researchers are also develop-  
114 ing LLMs for tabular data processing. Notable  
115 examples include TableGPT(Gong et al., 2020) and  
116 TABT5(Andrejczuk et al., 2022), which are trained  
117 for complex table-to-text generation tasks. Ad-  
118 ditionally, MediTabWang(Wang et al., 2023) has  
119 been specially developed for medical table predic-  
120 tion, showcasing the versatility of LLMs in han-  
121 dling structured data formats. Above successful  
122 large language models raise our beliefs that the

123 application value of tabular structured EHRs can  
124 be extensively mined and analyzed, offering deep  
125 clinical insights into patient care.

126 Furthermore, medical data is inherently multi-  
127 modal, making vision-and-language pre-training  
128 (VLP) a crucial technique for jointly understanding  
129 medical images and texts. Techniques like the Con-  
130 trastive Language-Image Pre-training (CLIP) (Rad-  
131 ford et al., 2021) treat the text caption as a linguistic  
132 representation of the image, pulling the image-text  
133 pair closer together in a latent space, have proven  
134 effective in aligning these pairs and showing sig-  
135 nificant benefits in various downstream applica-  
136 tions in the medical field, including image gener-  
137 ation, segmentation, detection, and classification.  
138 Although large-scale image-text pair datasets are  
139 essential in medical domain research, however, ex-  
140 isting large-scale datasets such as ROCO(Petersen  
141 et al., 2010), MedICat(Subramanian et al., 2020),  
142 FFA-IR(Li et al., 2021), and MIMIC-CXR(Johnson  
143 et al., 2019) and existing medical VLP(Tiu et al.,  
144 2022; Huang et al., 2021; Seibold et al., 2022; Pel-  
145 legrini et al., 2023) are predominantly focus on 2D  
146 images. While 2D slices can be adequate for learn-  
147 ing, 3D brain scans are crucial for brain disease  
148 diagnosis. Currently, there is no mature image-  
149 text pairing methodology for brain disease analysis.  
150 This paper aims to address this gap by introducing  
151 a novel pipline and establishing a Multimodality  
152 and Longitudinal dataset for neuroimaging studies.  
153 Specifically, our contributions are as follows:

- 154 • We collect comprehensive patient tabular data  
155 from ADNI, which includes demographic in-  
156 formation, biomarker measurements, cog-  
157 nitive assessments, and volumetric data. By  
158 analyzing this specialized clinical knowledge,  
159 we developed an annotation method that trans-  
160 forms tabular data into information-rich and  
161 fluent natural language.
- 162 • We present an encoder-decoder based model  
163 ADTabGPT(Medical tabular-to-text Genera-  
164 tive pre-trained transformers) that can be ap-  
165 plied to ADNI table-to-text generation. Mean-  
166 while, we collect and process a total of  
167 11107 volumetric T1-weighted MRI scans  
168 from ADNI as the image feature.
- 169 • To our best knowledge, this is the first work to  
170 explore the full utilization of multimodal and  
171 longitudinal EHRs for brain disease analysis.

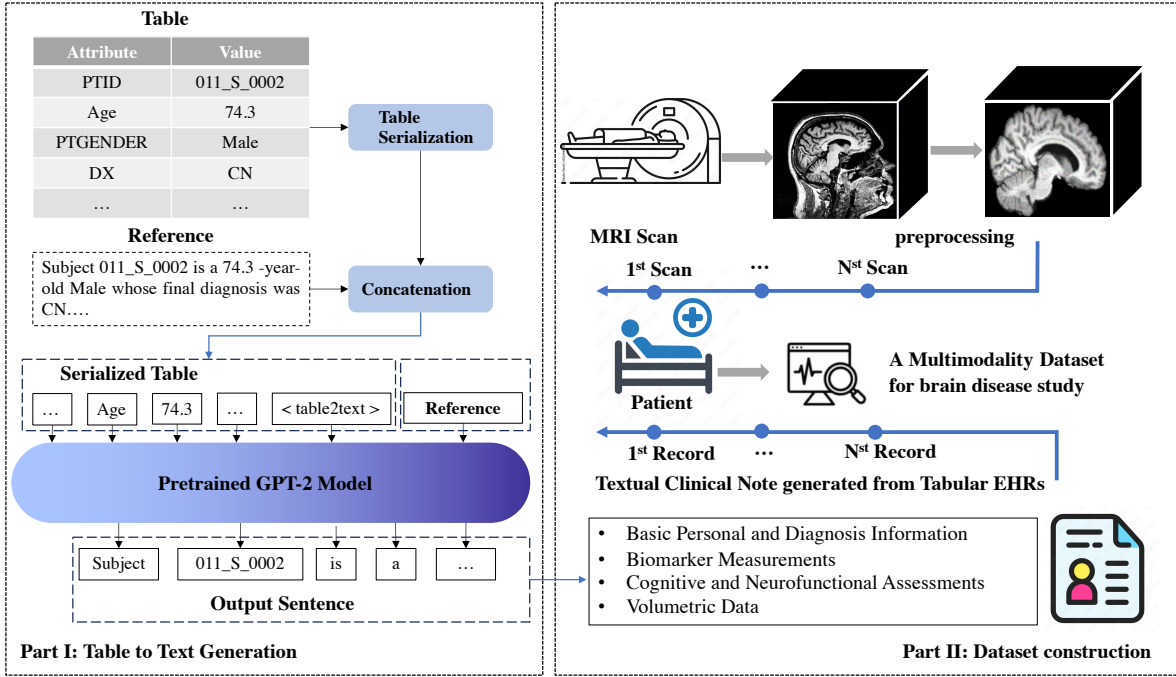


Figure 2: The overall architecture for constructing a multimodal and longitudinal Alzheimer’s Disease-related neuroimaging dataset. It encompasses two major parts: **Part I** transforms tabular clinical notes into natural language clinical reports; **Part II** preprocesses the corresponding MRI scans. Ultimately, these two modalities are combined.

## 2 Data Collection and Analysis

We design a four-step annotation process, as depicted in figure 2. Initially, we collect tabular EHRs and analysis the key variables, and then design ADTabGPT to convert them into natural language clinical reports, as illustrated in part I of Figure 2. Next, as shown in part II of Figure 2, we collect the corresponding MRI scans of patients from ADNI and undertake a series of preprocessing steps. Following above steps, we finally construct a multimodal and longitudinal neuroimaging EHR especially for Alzheimer’s disease.

### 2.1 Data Preparation

The ADNI is a consortium of universities and medical centers in the United States and Canada. It was established to develop standardized imaging techniques and biomarker procedures in Cognitive Normal(CN), MCI, and AD subjects. One of the major goals of ADNI is to create an accessible data repository that acquires clinical, cognitive, and biochemical data(Petersen et al., 2010). In addition to MRI imaging information, the ADNI provides an ocean of tabular data, allowing researchers and clinicians to explore the details such as demographic information(e.g., age, sex, educational level, etc);

biomarker measurements (e.g., allele producing the apolipoprotein E [APOE-ε4]); cognitive assessments (e.g., Mini-Mental State Examination, Clinical Dementia Rating Scale, etc); as well as volumetric data (e.g., metrics of the WholeBrain and Hippocampus).

This paper primarily focuses on the *AD-NIMERGE Table*, which merges several key variables from various case report forms and biomarker laboratory summaries across the ADNI protocols. The table encompasses 16,421 diagnostic records from 2,430 subjects, of which 2,409 have a diagnosis. the average age is  $73.2 \pm 7.0$  years, and the average educational attainment is  $16.1 \pm 2.8$  years. The data includes 4,020 diagnoses of CN individuals, 4,989 diagnoses of MCI, and 4,989 diagnoses of AD. The data comprises samples from three major racial groups: 2,143 White, 179 Black, and 58 Asian patients. Additionally, 50 samples include multiple racial backgrounds or are categorized as Unknown; American Indian/Alaskan Native; or Hawaiian/Other Pacific Islander. Gender-wise, females represent 52.4% of the subjects, totaling 1273, with the remainder being males. The ethnic distribution includes 2,302 non-Hispanic/Latino, 116 Hispanic/Latino, and 12 Unknown. From a

	CN group	MCI group	AD group
Gender (F/M)	475/354	324/448	345/463
Age(year)	71.4±6.8	73.0±7.5	74.4±7.5
Education(year)	16.6±2.5	15.9±2.8	15.6±2.8
APOE-ε4 <sub>0/1/2</sub>	511/202/20	411/226/56	374/274/134

Table 1: Basic demographic and biomarker statistics.

marital status perspective, there are 1,824 married, 269 widowed, 228 divorced, 99 never married, and 9 unspecified. Regarding the APOE-ε4 risk factor, 1,199 individuals do not carry the allele, 803 carry one copy, and 211 carry two copies. table 1 presents a basic demographic and biomarker statistics based on diagnostic. We also supplement the details of the distribution in the supplementary material. Additionally, ADNI provides a dictionary that elucidates the meaning of each variable. The details can also be found in the supplementary material table.

We collected 10387 T1-weighted MRI scans from ADNI, which includes 1510 AD scans (791 males, 719 females;  $76.27 \pm 7.86$  years), 3632 CN scans (1843 males, 1791 females;  $77.75 \pm 5.73$  years), and 5965 MCI scans (3758 males, 2198 females;  $75.47 \pm 7.53$  years). Following established works before (Zhang et al., 2021; Lyu et al., 2022), we performed a series of pre-processing steps as including bias field correction and skull stripping. All T1-weighted images are in NIFTI format and have been registered to the standard Montreal Neurological Institute (MNI) template using FSL-flirt linear registration tools and have a uniform view of  $197 \times 233 \times 189$ .

These T1-weighted MRI scans provide critical imaging perspectives for the analysis of brain diseases. For example, Post-mortem investigations have shown that structures in the medial temporal lobe, particularly the entorhinal cortex and hippocampus, are the first to change in AD and can be observed through MRI imaging techniques (Aramadaka et al., 2023). Fig 3 shows how brain morphology evolves with disease progression, from which we can observe a significant decrease in hippocampus volume.

### 3 ADTabGPT

#### 3.1 Problem Formulation

In this paper, we formulate each training instance  $(T, R)$  represented as a pair of linearized table  $T$  and their associated reference text  $R$ . The table  $T$

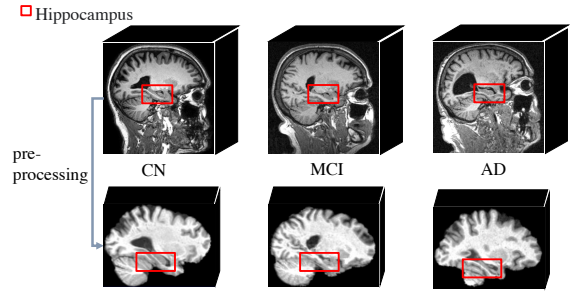


Figure 3: Brain morphology (hippocampus volume) contrast vary as a function of Alzheimer’s disease. The upper row are original MRI images and the lower are pre-processed (brain extraction and registration) images.

consists of a set of tabular data elements related to patients’ clinical notes, denoted as  $T = t_1, \dots, t_n$ , where each element  $t_i = a_i, v_i$  corresponds to an attribute (e.g., PTID)-value (e.g., 011\_S\_0002) pair and can be viewed as a sequence of words. Correspondingly,  $R = r_1, \dots, r_m$  represents the set of reference texts, with each  $r_i$  providing a narrative description that correlates with table  $T$ . The table-to-text model is expected to generate both fluent and faithful natural language descriptions of patients’ clinical information based on the given tables.

#### 3.2 Table Transformation

In contrast to the rich corpus data employed in Pre-trained Language Models (PLMs), tabular data present complex topology structures with sparse narrative descriptions, making them quite distinct from natural language representations. Fig.1 illustrates an example of tabular clinical notes and the human language set. To align with the sequential nature of language model, this paper employs a key-value pair template “PTID: 011\_S\_0002” as “PTID 011\_S\_0002” to structure the table into a sequence  $S$ . Subsequently, all of the key-value pairs are concatenated into a single sentence, that is, “PTID 011\_S\_0002 Age 74.3 PTGENDER Male ...”, while the corresponding textual description  $T$  is generated by another template: “Subject 011\_S\_0002 is a 74.3-year-old Male”. It should be noted that the original table may exhibit missing patient information, such as absent scan results or cognitive assessments, which are designated as “unknown”. Following the approach used in TableGPT (Gong et al., 2020), the structured table

S and the natural language description T are linked with a special token  $\langle table2text \rangle$  to encode the overall table information and signal the model to commence text generation. Another special token  $\langle endoftext \rangle$  marks the end of the entire sequence.

This methodology enables our model to encode the structured patients’ clinical notes and to learn to generate their natural language descriptions. The training objective of the language model is to maximize the likelihood of generating accurate textual clinical notes, that is,  $\max P(T | S)$ .

### 3.3 Annotation Challenges & Quality Evaluation

We find that one of the major challenges to generating patients’ clinical diagnostic reports from the given table is the presence of numerous missing values, primarily in biomarker measurements (e.g., ABETA, TAU, PTAU). To ensure the completeness and fluency of the generated reports, we set these missing value as “unknown”. For instance:

*"The subject’s genetic profile includes an ApoE4 status of unknown. Neuroimaging with FDG-PET shows average uptake in the angular, temporal, and posterior cingulate regions being unknown. Cerebrospinal fluid analysis reveals AA $\beta$  42 levels at unknown, total tau protein levels at unknown, and phosphorylated tau levels at unknown."*

Furthermore, to evaluate whether the clinical reports indeed reflect the patient’s potential for dementia, we split the annotated reports corpus (excluding the diagnosis results) into a training set (80%) for training the classifier and a test set (20%) for evaluation. We simply add a linear layer plus a binary softmax layer on the BERT model as the AD classifier. The accuracy of the classifier tested on the binary classification (CN, AD) reached 99%, and for the ternary classification (CN, MCI, AD) achieved 90%, shown as table 2. These results not only confirm the contribution of EHRs to AD diagnosis but also highlight the significant potential of ADNI tabular data for brain disease analysis.

Model	precision	recall	f1-score
BERT <sub>CN/AD</sub>	0.99	0.99	0.99
BERT <sub>CN/MCI/AD</sub>	0.90	0.89	0.90

Table 2: Performance of the BERT-based classifier.

## 4 Experiment

### 4.1 Baselines

We conduct experiments by fine-tuning following state-of-art text generation methods:

**Pointer Generator**(See et al., 2017) A LSTM-based seq2seq model incorporates a copy mechanism and was originally designed for text summarization. It has also been adapted for data-to-text applications(Gehrmann et al., 2018).

**BERT-to-BERT**(Rothe et al., 2020) A transformer-based encoder-decoder model initialized with BERT(Devlin et al., 2018).

**BART**(Lewis et al., 2019) A pre-trained denoising autoencoder with standard Transformer-based architecture model.

**T5**(Raffel et al., 2020) A transformer-based model is pre-trained to convert all textual language problems into text-to-text format and proves its effectiveness.

### 4.2 Evaluation Metrics

**Automatic Metrics** We employ two automatic metrics, BLEU(Papineni et al., 2002) and PAR-ENT(Dhingra et al., 2019). BLEU is widely used to evaluate machine-generated text quality and PAR-ENT is specifically designed for data-to-text tasks, which evaluates alignment by comparing n-grams from both the reference and generated texts to the source table.

**Human Evaluation** Since clinical reports require good readability and need to accurately reflect the patient’s various indicators, automatic metrics are not adequate to assess the quality of generated reports. We also perform human evaluation based on the following three criteria: 1) **fluency** indicates how well the report is structured; it evaluates whether the expressions are grammatical and fluent. 2) **Consistency** indicates whether the report is consistent with the data provided; it checks for discrepancies between the reported data and the actual measurements. 3) **Relevance** evaluates whether the report includes all necessary information pertinent to a clinical diagnosis, focusing on the inclusion of critical data and avoiding extraneous details. Above criteria ensure that each report is not only accurate but also practical for medical professionals diagnosing and treating patients in real-world clinical settings. Three experts were instructed to rate the three criteria on a scale from 1 to 5, where 1 denotes the worst and 5 represents the best possible score.

Model	BLUE-1/2/3	PARENT	Fluency	Consistency	Relevance
Pointer Generator	31.5/29.1/15.8	28.0	1.3	1.7	1.7
BERT-to-BERT	35.8/30.1/25.5	35.7	2.3	1.7	1.7
T5-small	56.6/40.6/30.6	60.3	3.3	2.0	2.3
T5-base	65.5/50.4/44.3	72.5	4.0	2.0	2.7
BART	76.0/65.0/55.8	88.1	4.7	3.0	3.7
ADTabGPT	<b>98.8/98.9/98.5</b>	<b>97.8</b>	<b>5.0</b>	<b>4.7</b>	<b>5.0</b>

Table 3: Results of automatic metrics and human evaluation.

### 4.3 Experiment Settings

We randomly split 16421 health records into train (70%), dev (15%) and test (15%) with no overlap. We download pre-trained GPT2 models from huggingface to avoid starting training from scratch. For optimizer, we adopt the OpenAI AdamW optimizer with 100 warm steps. The batchsize is set to 4 and we fine-tune the model 10 epochs with learning rate is set to  $2e-4$ . All experiments are conducted on a Nivida RTX TITAN GPU.

### 4.4 Results and Analysis

#### 4.4.1 Automatic Evaluation & Human Evaluation

As shown in Table 3, **first**, from an overall perspective, methods based on Large Language Models (i.e. T5 and BART) outperform the other approaches, with our ADTabGPT achieving the best results. Both metrics for methods based on LLM are scored highly. **Second**, we observed that our ADTabGPT-generated clinical notes almost identical to the references, achieving state-of-the-art results in both automatic and human evaluations. **Third**, we selected 200 generated clinical reports for human evaluation, and the results are presented in Table 3. Our method surpasses five baseline models across all three human-centric metrics. The most significant improvements are observed in consistency and relevance, demonstrating that our method can generate not only fluent diagnostic reports but also accurately reflect various patient indicators.

These results indicate that LLM are adept at handling table-to-text tasks, even in the highly specialized domain of neuroimaging. This reinforces our belief in the potential of using such techniques to mine valuable variables from ADNI tabular EHRs for Alzheimer’s disease analysis. Further, although the automatic evaluation shows high scores for the generated clinical reports, there are still existing issues, which will be analyzed in detail in the next

case study section.

#### 4.4.2 Case Study

We show in table 4 some clinical note examples generated by T5, BART, and our ADTabGPT. As we can see, both methods perform well in the initial sections of the diagnostic reports, Basic Personal Information. However, with longer documents, T5 and BART tend to produce various errors. The portions marked in orange indicate **hallucinations**, meaning the outputs cannot be verified against the source table data. The parts marked in red signify **more severe, multiple errors**. Beyond hallucinations, these include **value errors**, such as altering the patient’s measurements and test results, **grammatical error**, and **missing critical details**. This is particularly severe in the Cognitive and Neurofunctional Test Results section of T5’s outputs, where a significant amount of information is missing, affecting the understanding of patients’ diagnostic results. The sections marked in green highlight **anomalous symbols** in the diagnostic results, although the values are correct. This issue only appears in the BART-generated outputs. The occurrence of these problems may be due to the limited capacity of large models to handle long documents, resulting in errors when the patient’s diagnostic report is lengthy. Our ADTabGPT demonstrates perfect ability to generate fluent and faithful clinical reports in this example.

#### 4.4.3 EHR case

We provide an example of a patient’s diagnosis to detail our Multimodal and Longitudinal Neuroimaging EHR. As illustrated in Figure 4, we can observe the progression of this subject’s condition from both diagnostic reports and MRI imaging perspectives. In this case, the patient’s records span from 2006-01-19 to 2023-04-04, with the condition progressing from MCI to a confirmed diagnosis of AD.

Attribute	Value
PTID	002_S_4237
Age	80.9
Sex	Female
...	...

**ADTabGPT:(consistent with the reference)**

**Basic Personal Information:** Subject 002\_S\_4237 is a 80.9-year-old female who has completed 13 years of education. The ethnicity is Not Hisp/Latino and race is white. Marital status is never married. Initially diagnosed is early mild cognitive impairment, and on the date of 2007-10-14, the final diagnosis is mild cognitive impairment.

**Biomarker Measurements:** The subject's genetic profile includes an ApoE4 status of 0.0. Neuroimaging with FDG-PET shows average uptake in the angular, temporal, and posterior cingulate regions being 1.17185. Cerebrospinal fluid analysis reveals A $\beta$  42 levels at more than 1700, total tau protein levels at 302.1, and phosphorylated tau levels at 25.66.

**Cognitive and Neurofunctional Test Results:** The Mini-Mental State Examination score stands at 29.0. The Clinical Dementia Rating, sum of boxes, is 5.0. ADAS 11 and 13 scores are 12.0 and 12.0 respectively, with a score of 5.0 in delayed word recall. The Rey Auditory Verbal Learning Test results are as follows: immediate recall at 25.0, learning score at 9.0, forgetting score at 9.0, and percent forgetting at 9.0. Logical Memory test for delayed recall scored 6.0. The Digit Symbol Substitution test resulted in a score of Unknown. Trails B testing showed a score of 253.0. The modified Preclinical Alzheimer's Cognitive Composite scores using Digit Symbol Substitution and Trails B are -4.64725 and -6.38287 respectively. The Functional Activities Questionnaire rated the subject as 0.0.

**Imaging Data Points:** Under MRI conditions at a field strength of 3 Tesla, using Cross-Sectional FreeSurfer (5.1), the imaging data recorded includes ventricles volume at 92447.0, hippocampus volume at 6102.0, whole brain volume at 976304.0, entorhinal cortex volume at 3915.0, fusiform gyrus volume at 16367.0, and middle temporal area volume at 18784.0. The intracranial volume measured is 1516250.0.

**T5-base:**

**Basic Personal Information:** Subject 002\_S\_4237 is a 80.9-year-old Male who has completed 13 years of education. The ethnicity is Not Hisp/Latino and race is white. Marital status is never married. Initially diagnosed is early mild cognitive impairment, and on the date of 2007-10-14, the final diagnosis is mild cognitive impairment.

**Biomarker Measurement:** The subject's genetic profile includes an ApoE4 status of 0.0. Neuroimaging with FDG-PET shows average uptake in the angular, temporal, and posterior cingulate regions being dang gyrus. Cerebrospinal fluid analysis reveals A $\beta$  42 levels at spital to help wiyh the process of choosing he prefers the most.

**Cognitive and Neurofunctional Test Results:** The The Mini-Mental State Examination score stands at 4 and 13 in delay word recall. The Clinical Dementia Rating, sum of box, is 4. ADAS 11 and 13 scores are 9.0 and 9.0-PATH at 3.0.

Using Cross-Sectional FreeSurfer (5.1), **the Imaging Data Point:** Under MRI conditions are -4.64725 and 2-6.38287 respectively, with hippocampus volume at 6102.0. Logical Memory test at 6.0. The Digit Symbol Substitution test result in uncontrolled recall. Trails B testing showed obstructive Learning Test results are as follows: immediate recall at 225.0, learning score at 59.0 and percent forgetting at 7.0 in entorhinal cortex volume starting at 976304.0, fusiform gyrus density at 16367.0; the intracranial volume measured is 1516250.0

**BART:**

**Basic Personal Information:** Subject 002\_S\_4237 is a 80.9-year-old female who has completed 13 years of education. The ethnicity is Not Hisp/Latino and race is white. Marital status is never married. Initially diagnosed is early mild cognitive impairment, and on the date of 2007-10-14, the final diagnosis is mild cognitive impairment.

## BART:

**Biomarker Measurements:** The subject’s genetic profile includes an ApoE4 status of 0.0. Neuroimaging with FDG-PET shows average uptake in the angular, temporal, and posterior cingulate regions being 1.17185. Cerebrospinal fluid analysis reveals  $A\beta$  42 levels at more than 1700, total tau protein levels at 302.1, and phosphorylated tau levels at 25.66.

**Cognitive and Neurofunctional Test Results:** The Mini-Mental State Examination score stands at 29.0, with a score of 5.0 in elay word recall. The Rey Auditory Verbal Learning Test results are as follows: immediate recall at 25.0, learning score at 9.0%, forgetting score at 9.0, and percent forgetting at 9.0%. Logical Memory test for delayed recall scored 6.0%. The Digit Symbol Substitution test resulted in a score of Unknown. Trails B testing showed a score of 253.0 and a score for modified Preclinical Alzheimer’s Cognitive Composite scores of 253. The Functional Activities Questionnaire rated the subject as -6.38287.

**Imaging Data Points:** Under MRI conditions at a field strength of 3 Tesla, using Cross-Sectional FreeSurfer (5.1), the imaging data recorded includes ventricles volume at 92447.1, hippocampus volume at 6102.0, whole brain volume at 976304.0, entorhinal cortex volume at 3915.0, fusiform gyrus volume at 16367.0, and middle temporal area volume at 18784.0, The intracranial volume measured is 1516250.0.

Table 4: A sample tabular clinical diagnostic notes and the textual generated clinical diagnostic reports by our ADTabGPT and baslines. Text highlighted in orange indicates hallucinations, green text signifies errors involving anomalous symbols, and red text denotes multiple errors, including value errors, grammatical mistakes, and missing critical details.

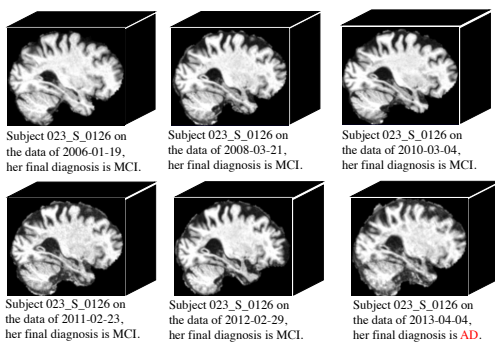


Figure 4: An example of patient’s multimodal and longitudinal EHR

## 5 Conclusion

Given the critical need for multimodal and longitudinal EHRs in brain-focused studies, we introduce the first vision-language brain dataset including 3D brain volume and comprehensive patient clinical notes. By collecting and analyzing ADNI tabular data, we developed a GPT-based method to transform them into information-rich and fluent natural language clinical reports. These reports encompass patients’ demographic information, biomarker measurements, cognitive assessments, and volumetric data. Using BERT for disease classification achieved an accuracy of 98.89%, which not only confirms the contribution of tabular EHRs to AD diagnosis but also highlights the significant poten-

tial of ADNI tabular data for brain disease analysis. Additionally, we collected 10,387 volumetric T1-weighted MRI scans from ADNI and adopted a series of preprocessing steps, which provide critical imaging perspectives for the analysis of brain diseases. Through the aforementioned annotation and preprocessing methods, we ultimately established a multimodal and longitudinal EHRs dataset that includes 3D brain image volumes and corresponding clinical notes. While ADNI dataset is publicly accessible, it requires approved access. To support future research in this area, we make our processing methods and code publicly available at <https://anonymous.4open.science/r/ADNI-table-to-Text-2EDB>

## Limitations

**Data scarcity** The ADNI dataset is extensive, and we have selected ADNIMERGE for our preliminary work. This table merges several key variables from various case report forms and biomarker laboratory summaries across the ADNI protocols. However, there are additional valuable tables, such as those detailing family history, drug history, and potential causes of AD (e.g., Frontotemporal Dementia, Major Depression, Parkinson’s Disease, Huntington’s Disease, etc.) Understanding these notes requires high levels of specialized knowledge. In our future work, we aim to integrate more of this

511	information to form a more comprehensive diagnostic report.	563
512		564
513	<b>Multi-scale features</b> A key distinction between	565
514	medical and natural images lies in the significance	566
515	of multi-scale features. Captions for natural images	567
516	are typically concise, providing an overall descrip-	568
517	tion. In contrast, medical reports consist of multi-	569
518	ple aspects and contain significantly more detailed	570
519	information, as illustrated in 1. These non-image	571
520	clinical informations are also pay a crucial role in	572
521	the medical domain, especially for AD diagnosis.	573
522	For instance, advanced age and specific genes, like	574
523	APOE4, are both significant risk factors for AD	575
524	but cannot be observed from images alone. Unlike	576
525	existing radiology reports, the clinical reports in	577
526	our dataset not only describe the volumetric aspects	578
527	of T1 scans but also include patients' demographic	579
528	information, biomarker measurements, and cogni-	580
529	tive assessments. How to effectively integrate these	581
530	clinical details into a unified embedding space and	582
531	align them effectively is a direction we will explore	583
532	in our future research.	584
533	<b>Inconsistency between pre-training and applica-</b>	585
534	<b>tion</b> A large number of research demonstrates that	586
535	CLIP's image encoder, initially pre-trained on nat-	587
536	ure images, also achieves impressive performance	588
537	in the medical domain. However, most existing	589
538	medical VLP models are designed to work with	590
539	2D images, which may significantly limit their ef-	
540	fectiveness in the neuroimaging domain, given the	
541	complex and sensitive nature of brain tissue. An	
542	important question arises: How can we effectively	
543	extend a 2D image encoder to extract features from	
544	3D medical? To address this, we will focus on de-	
545	veloping 3D VLP-driven models, specifically for	
546	brain analysis.	
547	<b>Medical VLP fairness</b> As previously reported in	
548	Section 2, there is significant imbalance in the dis-	
549	tribution of fine-grained attributes such as race, eth-	
550	nicity, and marital status within the data. Although	
551	the ADNI dataset is widely used, it was not primar-	
552	ily designed for fairness. Historical instances of	
553	bias in various technologies highlight the critical	
554	need for fairness in machine learning(Wang et al.,	
555	2022a; Dehdashtian et al., 2023). Large Vision-	
556	Language Pre-training models, which influence	
557	diagnostic and treatment decisions, can perpetu-	
558	ate healthcare disparities and result in adverse out-	
559	comes if they exhibit bias. Therefore, improving	
560	dataset quality and ensuring the fairness of model	
561	algorithms are not just ethical and legal imperatives,	
562	but also crucial for achieving healthcare equity(Luo	
	et al., 2024). While VLP models have significantly	563
	advanced various medical tasks and propelled the	564
	development of AI in healthcare, one of our key	565
	goals, as well as a direction for future efforts is	566
	to ensure these models provide fair and unbiased	567
	diagnostic results across different races, genders,	568
	and socioeconomic statuses.	569
	<b>Beyond image-text alignment</b> The philosophy of	570
	CLIP is centered on aligning different modalities,	571
	specifically images and text, by enabling the model	572
	to understand and establish meaningful connec-	573
	tions between visual and textual content. In the	574
	neuroimaging domain, images often involve vari-	575
	ous modalities such as MRI and PET scans. Specif-	576
	ically, structural MRI (sMRI) is used to depict the	577
	structure of the brain, while functional MRI (fMRI)	578
	reveals metabolic activity in the brain during spe-	579
	cific tasks(e.g., sensory, motor, cognitive functions,	580
	ect.). Each modality provides unique insights into	581
	different aspects of a patient's condition. Further-	582
	more, one of the most notable features of AD is	583
	hippocampal atrophy, however, in early mild cog-	584
	nitve impairment, structural changes are often not	585
	apparent and are typically inferred through func-	586
	tional assessments. In our future work, we plan	587
	to incorporate more modalities, such as functional	588
	MRI, combined with EHRs for comprehensive lon-	589
	gitudinal analysis of brain diseases.	590
	<b>References</b>	591
	2022. WWW '22: Proceedings of the ACM Web Con-	592
	ference 2022. Association for Computing Machinery,	593
	New York, NY, USA.	594
	Deepa Anand, Vanika Singhal, Dattesh D Shanbhag,	595
	Shriram KS, Uday Patil, Chitresh Bhushan, Kavitha	596
	Manickam, Dawei Gui, Rakesh Mullick, Avinash	597
	Gopal, et al. 2023. One-shot localization and seg-	598
	mentation of medical images with foundation models.	599
	<i>arXiv preprint arXiv:2310.18642.</i>	600
	Ewa Andrejczuk, Julian Martin Eisenschlos, Francesco	601
	Piccinno, Syrine Krichene, and Yasemin Altun. 2022.	602
	Table-to-text generation and pre-training with tabt5.	603
	<i>arXiv preprint arXiv:2210.09162.</i>	604
	Saikumar Aramadaka, Raam Mannam, Ra-	605
	jagopal Sankara Narayanan, Arpit Bansal, Vishnu R	606
	Yanamaladoddi, Sai Suseel Sarvepalli, and	607
	Shree Laya Vemula. 2023. Neuroimaging in	608
	alzheimer's disease for early diagnosis: a compre-	609
	hensive review. <i>Cureus</i> , 15(5).	610
	Sanoojan Baliyah, Fadillah A Maani, Santosh Sanjeev,	611
	and Muhammad Haris Khan. 2023. Exploring the	612
	transfer learning capabilities of clip in domain gen-	613
	eralization for diabetic retinopathy. In <i>International</i>	614

615		Yingjie Feng, Wei Chen, Xianfeng Gu, Xiaoyin Xu, and Min Zhang. 2023. Multi-modal semi-supervised evidential recycle framework for alzheimer’s disease classification. In <i>International Conference on Medical Image Computing and Computer-Assisted Intervention</i> , pages 130–140. Springer.	669
616			670
617	Mrinal Kanti Baowaly, Chia-Ching Lin, Chao-Lin Liu, and Kuan-Ta Chen. 2019. Synthesizing electronic health records using improved generative adversarial networks. <i>Journal of the American Medical Informatics Association</i> , 26(3):228–241.		671
618			672
619			673
620			674
621			
622	Elliot Bolton, David Hall, Michihiro Yasunaga, Tony Lee, Chris Manning, and Percy Liang. 2022. Biomedlm: a domain-specific large language model for biomedical text. <i>Stanford CRFM Blog</i> .		675
623			676
624			677
625			678
626	Anna L Buczak, Steven Babin, and Linda Moniz. 2010. Data-driven approach for creating synthetic electronic medical records. <i>BMC medical informatics and decision making</i> , 10:1–28.		679
627			680
628			681
629			682
630	Hongmin Cai, Zhixuan Zhou, Defu Yang, Guorong Wu, and Jiazhou Chen. 2023. Discovering brain network dysfunction in alzheimer’s disease using brain hypergraph neural network. In <i>International Conference on Medical Image Computing and Computer-Assisted Intervention</i> , pages 230–240. Springer.		683
631			684
632			685
633			686
634			687
635			688
636	Maria C Carrillo and Eliezer Masliah. 2023. Nia-aa revised clinical criteria for alzheimer’s disease. In <i>Alzheimer’s Association International Conference</i> . ALZ.		689
637			690
638			691
639			692
640	Qiuhui Chen, Xinyue Hu, Zirui Wang, and Yi Hong. 2023. Medblip: Bootstrapping language-image pre-training from 3d medical images and texts. <i>arXiv preprint arXiv:2305.10799</i> .		693
641			694
642			695
643			696
644	Edward Choi, Siddharth Biswal, Bradley Malin, Jon Duke, Walter F Stewart, and Jimeng Sun. 2017. Generating multi-label discrete patient records using generative adversarial networks. In <i>Machine learning for healthcare conference</i> , pages 286–305. PMLR.		697
645			698
646			699
647			700
648			701
649	Sepehr Dehdashtian, Lan Wang, and Vishnu Boddeti. 2023. Fairvlm: Mitigating bias in pre-trained vision-language models. In <i>The Twelfth International Conference on Learning Representations</i> .		702
650			703
651			704
652			705
653	Jacob Devlin, Ming-Wei Chang, Kenton Lee, and Kristina Toutanova. 2018. Bert: Pre-training of deep bidirectional transformers for language understanding. <i>arXiv preprint arXiv:1810.04805</i> .		706
654			707
655			708
656			709
657	Bhuwan Dhingra, Manaal Faruqui, Ankur Parikh, Ming-Wei Chang, Dipanjan Das, and William W Cohen. 2019. Handling divergent reference texts when evaluating table-to-text generation. <i>arXiv preprint arXiv:1906.01081</i> .		710
658			711
659			712
660			713
661			714
662	Björn Engelmann, Timo Breuer, and Philipp Schaefer. 2023. <a href="#">Simulating users in interactive web table retrieval</a> . In <i>Proceedings of the 32nd ACM International Conference on Information and Knowledge Management</i> , CIKM ’23, page 3875–3879, New York, NY, USA. Association for Computing Machinery.		715
663			716
664			717
665			718
666			719
667			720
668			721
			722
			723

724	Alistair EW Johnson, Tom J Pollard, Seth J Berkowitz,	transformer: Classification of alzheimer’s disease	781
725	Nathaniel R Greenbaum, Matthew P Lungren, Chih-	via vision transformer. In <i>Proceedings of the 15th</i>	782
726	ying Deng, Roger G Mark, and Steven Horng.	<i>International Conference on PErvasive Technologies</i>	783
727	2019. MIMIC-CXR, a de-identified publicly available	<i>Related to Assistive Environments</i> , pages 463–468.	784
728	database of chest radiographs with free-text reports.		
729	<i>Scientific data</i> , 6(1):317.		
730	Mindy J Katz, Richard B Lipton, Charles B Hall,	Scott McLachlan, Kudakwashe Dube, and Thomas Gal-	785
731	Molly E Zimmerman, Amy E Sanders, Joe Verghese,	agher. 2016. Using the caremap with health inci-	786
732	Dennis W Dickson, and Carol A Derby. 2012. Age-	dents statistics for generating the realistic synthetic	787
733	specific and sex-specific prevalence and incidence of	electronic healthcare record. In <i>2016 IEEE Interna-</i>	788
734	mild cognitive impairment, dementia, and alzheimer	<i>tional Conference on Healthcare Informatics (ICHI)</i> ,	789
735	dementia in blacks and whites: a report from the ein-	pages 439–448. IEEE.	790
736	stein aging study. <i>Alzheimer Disease &amp; Associated</i>		
737	<i>Disorders</i> , 26(4):335–343.	Michael B Miller, August Yue Huang, Junho Kim, Zi-	791
738	Yilin Leng, Wenju Cui, Chen Bai, Zirui Chen, Yanyan	nan Zhou, Samantha L Kirkham, Eduardo A Maury,	792
739	Zheng, and Jian Zheng. 2023. Dynamic structural	Jennifer S Ziegenfuss, Hannah C Reed, Jennifer E	793
740	brain network construction by hierarchical prototype	Neil, Lariza Rento, et al. 2022. Somatic genomic	794
741	embedding gcn using t1-mri. In <i>International Con-</i>	changes in single alzheimer’s disease neurons. <i>Na-</i>	795
742	<i>ference on Medical Image Computing and Computer-</i>	<i>ture</i> , 604(7907):714–722.	796
743	<i>Assisted Intervention</i> , pages 120–130. Springer.		
744	Mike Lewis, Yinhan Liu, Naman Goyal, Marjan	Kishore Papineni, Salim Roukos, Todd Ward, and Wei-	797
745	Ghazvininejad, Abdelrahman Mohamed, Omer Levy,	Jing Zhu. 2002. Bleu: a method for automatic evalu-	798
746	Ves Stoyanov, and Luke Zettlemoyer. 2019. Bart: De-	ation of machine translation. In <i>Proceedings of the</i>	799
747	noising sequence-to-sequence pre-training for natural	<i>40th annual meeting of the Association for Computa-</i>	800
748	language generation, translation, and comprehension.	<i>tional Linguistics</i> , pages 311–318.	801
749	<i>arXiv preprint arXiv:1910.13461</i> .		
750	Junnan Li, Dongxu Li, Silvio Savarese, and Steven Hoi.	Chantal Pellegrini, Matthias Keicher, Ege Özsoy, Petra	802
751	2023. Blip-2: Bootstrapping language-image pre-	Jiraskova, Rickmer Braren, and Nassir Navab. 2023.	803
752	training with frozen image encoders and large lan-	Xplainer: From x-ray observations to explainable	804
753	guage models. In <i>International conference on ma-</i>	zero-shot diagnosis. In <i>International Conference on</i>	805
754	<i>chine learning</i> , pages 19730–19742. PMLR.	<i>Medical Image Computing and Computer-Assisted</i>	806
755	Junnan Li, Dongxu Li, Caiming Xiong, and Steven	<i>Intervention</i> , pages 420–429. Springer.	807
756	Hoi. 2022. Blip: Bootstrapping language-image pre-		
757	training for unified vision-language understanding	Ronald Carl Petersen, Paul S Aisen, Laurel A Beck-	808
758	and generation. In <i>International conference on ma-</i>	ett, Michael C Donohue, Anthony Collins Gamst,	809
759	<i>chine learning</i> , pages 12888–12900. PMLR.	Danielle J Harvey, CR Jack Jr, William J Ja-	810
760	Mingjie Li, Wenjia Cai, Rui Liu, Yuetian Weng, Xi-	gust, Leslie M Shaw, Arthur W Toga, et al. 2010.	811
761	aoyun Zhao, Cong Wang, Xin Chen, Zhong Liu,	Alzheimer’s disease neuroimaging initiative (adni)	812
762	Caineng Pan, Mengke Li, et al. 2021. FFA-IR: Towards	clinical characterization. <i>Neurology</i> , 74(3):201–209.	813
763	an explainable and reliable medical report genera-		
764	tion benchmark. In <i>Thirty-fifth conference on neural</i>	Alec Radford, Jong Wook Kim, Chris Hallacy, Aditya	814
765	<i>information processing systems datasets and bench-</i>	Ramesh, Gabriel Goh, Sandhini Agarwal, Girish Sas-	815
766	<i>marks track (round 2)</i> .	try, Amanda Askell, Pamela Mishkin, Jack Clark,	816
767	Wei Liang, Kai Zhang, Peng Cao, Pengfei Zhao, Xiaoli	et al. 2021. Learning transferable visual models from	817
768	Liu, Jinzhu Yang, and Osmar R Zaiane. 2023. Model-	natural language supervision. In <i>International confer-</i>	818
769	ing alzheimers’ disease progression from multi-task	<i>ence on machine learning</i> , pages 8748–8763. PMLR.	819
770	and self-supervised learning perspective with brain		
771	networks. In <i>International Conference on Medical</i>	Colin Raffel, Noam Shazeer, Adam Roberts, Katherine	820
772	<i>Image Computing and Computer-Assisted Interven-</i>	Lee, Sharan Narang, Michael Matena, Yanqi Zhou,	821
773	<i>tion</i> , pages 310–319. Springer.	Wei Li, and Peter J Liu. 2020. Exploring the lim-	822
774	Yan Luo, Min Shi, Muhammad Osama Khan, Muham-	its of transfer learning with a unified text-to-text	823
775	mad Muneeb Afzal, Hao Huang, Shuaihang Yuan,	transformer. <i>Journal of machine learning research</i> ,	824
776	Yu Tian, Luo Song, Ava Kouhana, Tobias Elze,	21(140):1–67.	825
777	et al. 2024. Fairclip: Harnessing fairness in vision-	Sascha Rothe, Shashi Narayan, and Aliaksei Severyn.	826
778	language learning. <i>arXiv preprint arXiv:2403.19949</i> .	2020. Leveraging pre-trained checkpoints for se-	827
779	Yanjun Lyu, Xiaowei Yu, Dajiang Zhu, and Lu Zhang.	quence generation tasks. <i>Transactions of the Associ-</i>	828
780	2022. Classification of alzheimer’s disease via vision	<i>ation for Computational Linguistics</i> , 8:264–280.	829
		Abigail See, Peter J Liu, and Christopher D Man-	830
		ning. 2017. Get to the point: Summarization	831
		with pointer-generator networks. <i>arXiv preprint</i>	832
		<i>arXiv:1704.04368</i> .	833
		Constantin Seibold, Simon Reiß, M Saquib Sarfraz,	834
		Rainer Stiefelhagen, and Jens Kleesiek. 2022. Break-	835
		ing with fixed set pathology recognition through	836

837	report-guided contrastive training. In <i>International Conference on Medical Image Computing and Computer-Assisted Intervention</i> , pages 690–700. Springer.	Lu Zhang, Li Wang, Jean Gao, Shannon L Risacher, Jingwen Yan, Gang Li, Tianming Liu, Dajiang Zhu, Alzheimer’s Disease Neuroimaging Initiative, et al. 2021. Deep fusion of brain structure-function in mild cognitive impairment. <i>Medical image analysis</i> , 72:102082.	891
838			892
839			893
840			894
841	Sanjay Subramanian, Lucy Lu Wang, Sachin Mehta, Ben Bogin, Madeleine van Zuylen, Sravanthi Parasa, Sameer Singh, Matt Gardner, and Hannaneh Hajishirzi. 2020. Medicat: A dataset of medical images, captions, and textual references. <i>arXiv preprint arXiv:2010.06000</i> .	Ziqi Zhang, Chao Yan, Diego A Mesa, Jimeng Sun, and Bradley A Malin. 2020. Ensuring electronic medical record simulation through better training, modeling, and evaluation. <i>Journal of the American Medical Informatics Association</i> , 27(1):99–108.	895
842			896
843			897
844			898
845			899
846			900
847	Yuan Sui, Mengyu Zhou, Mingjie Zhou, Shi Han, and Dongmei Zhang. 2023. Evaluating and enhancing structural understanding capabilities of large language models on tables via input designs. <i>arXiv preprint arXiv:2305.13062</i> .	Rong Zhou, Houliang Zhou, Brian Y Chen, Li Shen, Yu Zhang, and Lifang He. 2023a. Attentive deep canonical correlation analysis for diagnosing alzheimer’s disease using multimodal imaging genetics. In <i>International Conference on Medical Image Computing and Computer-Assisted Intervention</i> , pages 681–691. Springer.	901
848			902
849			903
850			904
851			905
852	Ekin Tiu, Ellie Talius, Pujan Patel, Curtis P Langlotz, Andrew Y Ng, and Pranav Rajpurkar. 2022. Expert-level detection of pathologies from unannotated chest x-ray images via self-supervised learning. <i>Nature Biomedical Engineering</i> , 6(12):1399–1406.	Yanjie Zhou, Youhao Li, Feng Zhou, Yong Liu, and Liyun Tu. 2023b. Learning with domain-knowledge for generalizable prediction of alzheimer’s disease from multi-site structural mri. In <i>International Conference on Medical Image Computing and Computer-Assisted Intervention</i> , pages 452–461. Springer.	906
853			907
854			908
855			909
856			910
857	Ashish Vaswani, Noam Shazeer, Niki Parmar, Jakob Uszkoreit, Llion Jones, Aidan N Gomez, Łukasz Kaiser, and Illia Polosukhin. 2017. Attention is all you need. <i>Advances in neural information processing systems</i> , 30.		911
858			912
859			913
860			914
861			915
862	Junyang Wang, Yi Zhang, and Jitao Sang. 2022a. Fairclip: Social bias elimination based on attribute prototype learning and representation neutralization. <i>arXiv preprint arXiv:2210.14562</i> .	<b>appendix</b>	916
863		<b>A Related Work</b>	917
864		<b>EHRs Generation</b> EHRs are a longitudinal record that encompass a patient’s health information. Early works on generating EHRs were predominantly ruled-based(Buczak et al., 2010; McLachlan et al., 2016). However, powered by neural networks, recent advancements have seen the adoption of deep learning models and artificial intelligence (AI), which have significantly enhanced this process. One pioneering innovation was MedGAN proposed by(Choi et al., 2017), aiming to generating multi-label discrete patient records using generative adversarial networks (GANs) models (Goodfellow et al., 2020). Following this development, numerous studies have focused on improving medical text generation(Guan et al., 2018; Baowaly et al., 2019; Zhang et al., 2020). However, most EHRs only focus on static, single-modal EHRs and overlook the representations of imaging information. To the best of our knowledge, we are the first to focus on building a multimodal and longitudinal EHRs dataset for brain disease analysis.	918
865			919
866	Zifeng Wang, Chufan Gao, Cao Xiao, and Jimeng Sun. 2023. Meditab: Scaling medical tabular data predictors via data consolidation, enrichment, and refinement.		920
867			921
868			922
869			923
870	Zifeng Wang, Zhenbang Wu, Dinesh Agarwal, and Jimeng Sun. 2022b. Medclip: Contrastive learning from unpaired medical images and text. <i>arXiv preprint arXiv:2210.10163</i> .		924
871			925
872			926
873			927
874	Yongjian Wu, Yang Zhou, Jiya Saiyin, Bingzheng Wei, Maode Lai, Jianzhong Shou, Yubo Fan, and Yan Xu. 2023. Zero-shot nuclei detection via visual-language pre-trained models. In <i>International Conference on Medical Image Computing and Computer-Assisted Intervention</i> , pages 693–703. Springer.		928
875			929
876			930
877			931
878			932
879			933
880	Xiaowei Yu, Lu Zhang, Yanjun Lyu, Tianming Liu, and Dajiang Zhu. 2023. Supervised deep tree in alzheimer’s disease. In <i>2023 IEEE 20th International Symposium on Biomedical Imaging (ISBI)</i> , pages 1–5. IEEE.	<b>Vision-Language Models</b> The integration of vision and language in deep learning, exemplified by models such as CLIP, trained on a large scale of paired image-text multimodal data, represents	934
881			935
882			936
883			937
884			938
885	Lu Zhang, Saiyang Na, Tianming Liu, Dajiang Zhu, and Junzhou Huang. 2023. Multimodal deep fusion in hyperbolic space for mild cognitive impairment study. In <i>International Conference on Medical Image Computing and Computer-Assisted Intervention</i> , pages 674–684. Springer.		939
886			940
887			941
888			
889			
890			

942 a significant advancement in aligning visual in- 994  
943 formation with textual descriptions in AI. Boot- 995  
944 strapping Language-Image Pre-training (BLIP)(Li 996  
945 et al., 2022) introduces a novel multimodal, unified 997  
946 encoder-decoder framework to learn from noisy 998  
947 image-text pairs. Further enhancing this work, 999  
948 BLIP-2 (Li et al., 2023) proposed a lightweight  
949 querying transformer, achieving state-of-the-art  
950 performance on various vision-language tasks with  
951 considerably fewer trainable parameters.

952 These success of CLIP-like models have  
953 achieved great success in many downstream com-  
954 puter vision applications. Hence, it is intuitive  
955 to understanding complex medical imaging using  
956 VLP models, which has also led to rapid advance-  
957 ments in various medical domain (e.g., Chest X-  
958 ray, multi-organ CT, Brest Histology). For in-  
959 stance, Xplainer (Pellegrini et al., 2023) leverages  
960 the CLIP to align the of X-Ray scans and clinical  
961 radiology reports representations close in latent  
962 space for zero-shot diagnosing pathologies. Med-  
963 CLIP(Wang et al., 2022b) employs inter-report se-  
964 mantical correlation as the soft optimization target  
965 for the alignment between X-Ray medical image  
966 and text. CoOPLVT (Baliah et al., 2023) investi-  
967 gate CLIP’s transfer learning capabilities and its  
968 potential for cross-domain generalization in dia-  
969 betic retinopathy (DR) classification. Wu et al.(Wu  
970 et al., 2023) proposed a zero-shot nuclei detection  
971 framework based on VLP models by directly using  
972 automatic text prompts.

973 Above research demonstrate that CLIP’s image  
974 encoder, initially pre-trained on nature images, also  
975 achieves impressive performance in the medical do-  
976 main. However, most existing medical VLP mod-  
977 els are designed based on 2D images, for 3D MRI  
978 images, (Anand et al., 2023) taking them into 2D  
979 slices. The brain, with its complex features, espe-  
980 cially for brain disease diagnosis, is sensitive to  
981 even minor tissue changes, and slicing may com-  
982 promise these crucial features. MedBLIP (Chen  
983 et al., 2023) extracts and fuses 3D medical volume  
984 images, aligning them with text features in a com-  
985 mon space using BioMedLM (Bolton et al., 2022),  
986 and then fine-tunes the alignment using LoRA(Hu  
987 et al., 2021). However, they only utilizes patient  
988 age and a limited number of cognitive test results  
989 as textual descriptions, missing out on a wealth of  
990 valuable information contained in ADNI EHRs.

991 One major challenge in applying VLP for brain  
992 analysis lies in the scarcity of available image-text  
993 pair datasets. Therefore, this paper aims to develop

a multimodal and longitudinal EHRs that includes  
3D brain image volumes and corresponding clinical  
notes for brain disease studies. We expect that  
this dataset not only enhances the quality but also  
broadens the horizon for research in the brain dis-  
ease domain.

## 994 B Data Descriptions 1000

ADNI provides a dictionary that clarifies the mean-  
ing of each variable. To supplement the details,  
Table 5 presents information about the variables  
along with their descriptions. We also include an  
example in this table to illustrate their application.  
Table 5

## 1001 C Data Distribution 1007

To supplement the details for our neuroimaging  
EHR in the main paper, we present additional anal-  
yses. Figures 5a and 5b illustrate the distribution  
of gender and marital status, respectively. Figure  
5c depicts the distribution of initial and final diag-  
noses, while Figures 5d and 5e show the distribu-  
tions of racial and ethnic backgrounds. Figure 5f  
presents the distribution of the APOE4 gene allele  
carriers.

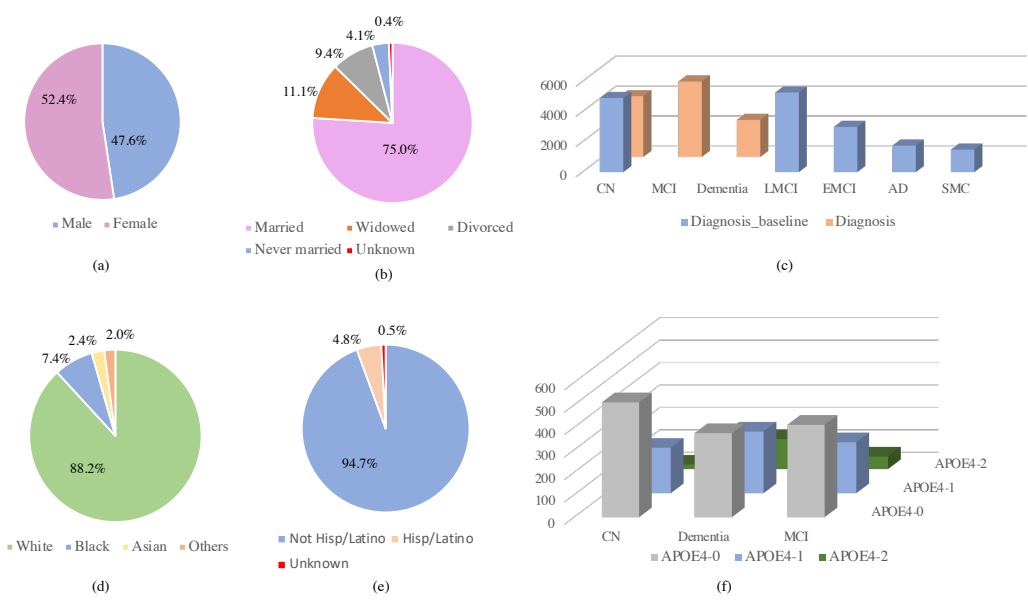


Figure 5: (a) distribution of gender, (b) distribution of marital status, (c) distribution of initial and final diagnoses, (d) distributions of racial, (e) distributions of ethnic, (f) distribution of the APOE4 gene allele carriers

Information	Information Description	Example
PTID	Original study protocol	011_S_0002
Age	Age	74.3
PTGENDER	Sex	Male
PTEDUCAT	Education	16
PTETHCAT	Ethnicity	Not Hisp/Latino
PTRACCAT	Race	White
PTMARRY	Marital	Married
EXAMDATE	Date	09/08/2005
DX_bl	Baseline DX	CN
DX	DX	CN
APOE4	ApoE4	0
FDG	Average FDG-PET of angular, temporal, and posterior cingulate.	1.33615
ABETA	CSF ABETA	741.5
TAU	CSF TAU	239.7
PTAU	CSF PTAU	22.83
CDRSB	CDR	0
ADAS11	ADAS 11	10.67
ADAS13	ADAS 13	18.67
ADASQ4	ADAS Delayed Word Recall	5
MMSE	MMSE	28
RAVLT_immediate	RAVLT Immediate (sum of 5 trials)	44
RAVLT_learning	RAVLT Learning (trial 5 - trial 1)	4
RAVLT_forgetting	RAVLT Forgetting (trial 5 - delayed)	6
RAVLT_perc_forgetting	RAVLT Percent Forgetting	54.5455
LDELTOTAL	Logical Memory - Delayed Recall	10
DIGITSCOR	Digit Symbol Substitution	34
TRABSCOR	Trails B	112
mPACCdigit	ADNI modified Preclinical Alzheimer's Cognitive Composite (PACC) with Digit Symbol Substitution	-4.31028
mPACCtrailsB	ADNI modified Preclinical Alzheimer's Cognitive Composite (PACC) with Trails B	-4.11443
FAQ	FAQ	0
FLDSTRENG	MRI Field Strength	1.5 Tesla MRI
FSVERSION	FSVERSION	Cross-Sectional FreeSurfer (FreeSurfer Version 4.3)
Ventricles	UCSF Ventricles	118233
Hippocampus	UCSF Hippocampus	8336
WholeBrain	UCSF WholeBrain	1229740
Entorhina	UCSF Entorhinal	4117
Fusiform	UCSF Fusiform	16559
MidTemp	UCSF Med Temo	27936
ICV	UCSF ICV	1984660

Table 5: This table presents information from the ADNIMERGE table and its corresponding descriptions from official ADNIMERGE-DICTIONARY, detailing patient data in the ADNI study. Each category of information is highlighted with a specific color: 7 pieces of basic personal and 3 pieces of diagnosis information, 5 biomarker measurements, 15 cognitive and neurofunctional test results, 7 imaging data points, and 2 additional related indicators(MRI Field Strength and FS VERSION). Each entry in the table includes an example for clearer understanding.